Decadal Survey Testbed Commissioning Roadmap: Demonstrating Technology for Imaging New Worlds

Garreth Ruane, Brendan Crill, Keith Patterson, Camilo Mejia Prada, Byoung-Joon Seo, and Nick Siegler

Jet Propulsion Laboratory, California Institute of Technology, Pasadena, CA

Version date: April 25, 2019

Introduction

The Decadal Survey Testbed (DST) aims to the demonstrate the coronagraph technologies required to directly image and characterize Earth-like exoplanets with future space telescopes; e.g. the Habitable Exoplanet Explorer (HabEx)[1] and the Large Ultra-violet, Optical, Infrared (LUVOIR) Surveyor[2] mission concepts. The DST is a state-of-the-art coronagraph instrument with high thermal and vibrational stability located in the High Contrast Imaging Testbed (HCIT) laboratory at NASA's Jet Propulsion Laboratory (JPL). The commissioning of the DST is managed by the NASA Exoplanet Exoploration Program (ExEP) office. This document outlines goals of the DST and the experiments planned to commission the DST in preparation for NASA/SAT funded coronagraph demonstrations and support of future direct imaging missions.

The DST (see Fig. 1) is a new, advanced testbed that consists of a stellar source simulator, two deformable mirrors (DMs) for wavefront control, coronagraph masks, a wavefront sensor, and an imaging camera. The DST's opto-mechanical design minimizes disturbances from the laboratory and local environment. At its foundation, the DST consists of a carbon-fiber optical table that is highly stable to thermal fluctuations and includes active temperature control. Vibration isolators reduce the sensitivity to seismic and laboratory vibrations. An active steering mirror can actively correct for residual tip/tilt errors while the two DMs correct other imperfections in the optical wavefront. All of the optics are highly polished and reflective where possible to minimize wavelength dependent aberrations. The entire testbed is housed inside of a 12-meter long vacuum chamber to eliminate effects of the atmosphere.

The DST is designed to primarily address technology gap CG-2 in the Technology Plan Appendix[3]: Coronagraph masks and optics capable of creating circularly symmetric dark regions in the focal plane enabling raw contrasts $\leq 10^{-10}$, with minimal contribution from polarization aberration, IWA $< 3\,\lambda/D$ for unobscured apertures, throughput $\geq 10\%$, and bandwidth $\geq 10\%$ on obscured and segmented pupils in a simulated dynamic vacuum environment.

When the commissioning requirements are met, the DST will be capable of demonstrating the following:

1. **Raw contrast.** DST will demonstrate the ability to efficiently image an exoplanet with one Earth radius ($R_\oplus$) at one astronomical unit (au) from its host star. Such a planet is approximately 10^{-10} times fainter than its host star. Thus, the nominal goal for commissioning is a raw contrast on the order of 10^{-10} in an annular region 3-10 λ/D with a spectral bandwidth of $\Delta\lambda/\lambda \geq 0.1$.

2. **High-order wavefront sensing & control.** DST will be able to sense and correct differential wavefront aberrations of 10-100 pm RMS at spatial frequencies up to 30 cycles per pupil diameter. Controlling the wavefront error (WFE) over this spatial bandwidth is critical for maintaining the dark hole for extended periods of time with realistic disturbances, especially at the spatial frequencies that have a strong influence within the optimized field of view. This need is also called out in technology gap CG-5[3].

3. **Deformable mirror (DM) drift.** DST will study the effects of the stability of two DM technologies and demonstrate that the surface deformations may be controlled at a sufficient cadence, if necessary.

4. **Segment phasing errors.** DST will demonstrate the capability to sense and correct segment-to-segment phasing errors in closed loop using a wavefront sensor.

5. **Robust coronagraphs.** DST will demonstrate coronagraphs that are passively insensitive to changes in low order aberrations on the order of 100 pm RMS.

6. **Throughput.** DST will demonstrate coronagraphs with improved throughput with respect to basic Lyot coronagraphs.

7. **Field of view.** DST will demonstrate outer working angles that approach the limits of the DM control authority: $\sim N_{\text{act}}\lambda_{\text{min}}/2D$, where N_{act} is the number of actuators across a beam of diameter D and λ_{min} is the minimum wavelength.

8. **Instantaneous bandwidths.** DST will demonstrate coronagraphs with extended instantaneous bandwidth up to and potentially beyond $\Delta\lambda/\lambda = 0.2$. This allows optical spectroscopy over $\lambda = 450\text{-}1000$ nm in four or fewer sub-bands.
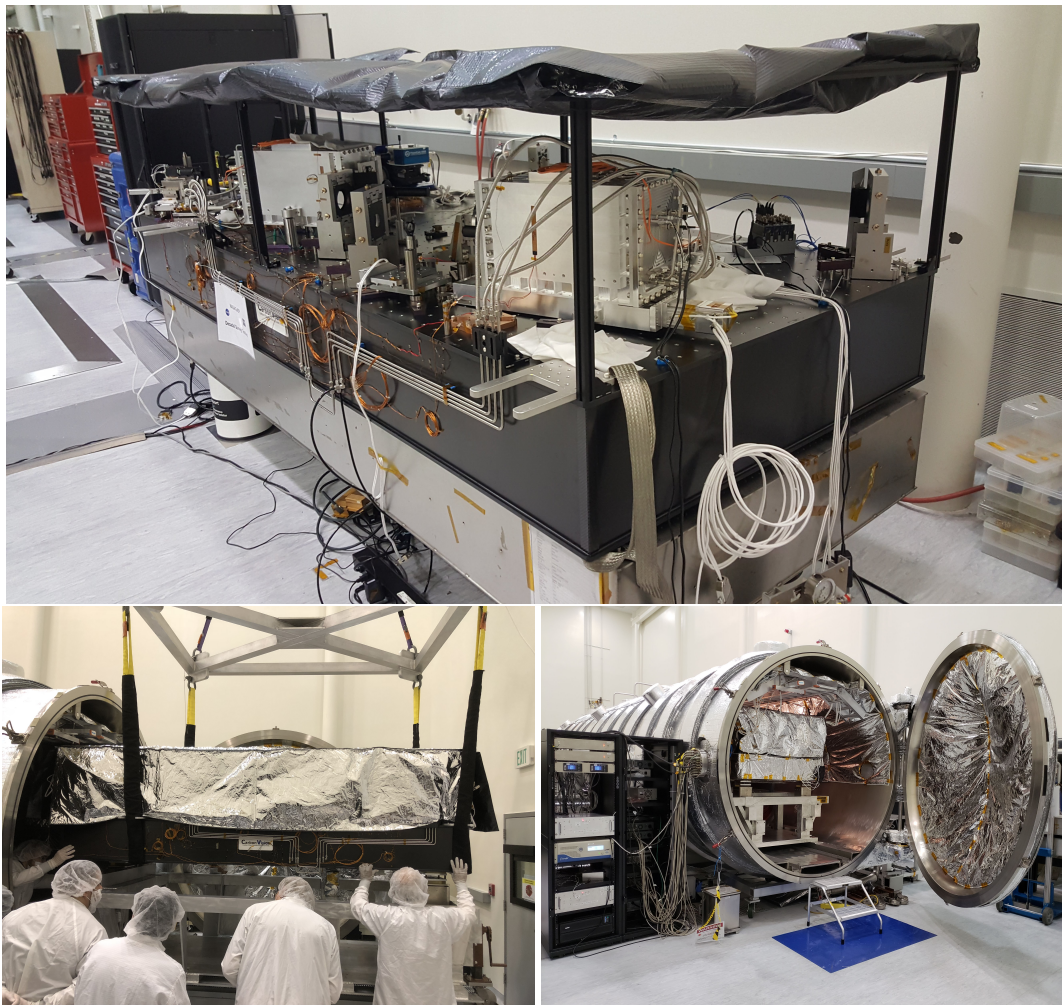
Figure 1. Photos of the DST (*top*) during alignment and integration, and (*bottom left*) while being installed, (*bottom right*) after installation in the vacuum chamber.

## Summary of DST commissioning phases

Phase 1: Coronagraph testing with an unobscured pupil
#### Phase 1a: Demonstrating the testbed noise floor

- Goal: Achieve raw contrast on the order of 10^{-10} with a Lyot coronagraph in a 360° dark hole, 3-10 λ/D, and a spectral bandwidth of $\Delta\lambda/\lambda = 0.1$.

- Use the optical layout in Fig. 2.

- Use circular unobscured pupil, a focal plane mask with a circular occulting spot, and an annular Lyot stop.

- Maintain static environment to study the natural testbed stability and temporal evolution of the dark hole region.

Phase 1b: DM performance comparison

- Compare PMN and MEMS DMs, respectively from Xinetics and Boston Micromachines, to quantify tradeoffs between DM technologies and inform future investigators and the WFIRST mission regarding the DM performance trades.

- Use MEMS DMs instead of the Xinetics DMS while minimizing changes to the testbed layout (see Fig. 3).

- Goal: Achieve $<10^{-9}$ raw contrast levels in a 360° dark hole, 3-10 λ/D, and a spectral bandwidth of $\Delta\lambda/\lambda = 0.1$.

- Repeat above experiments with WFIRST pupil and coronagraph masks.
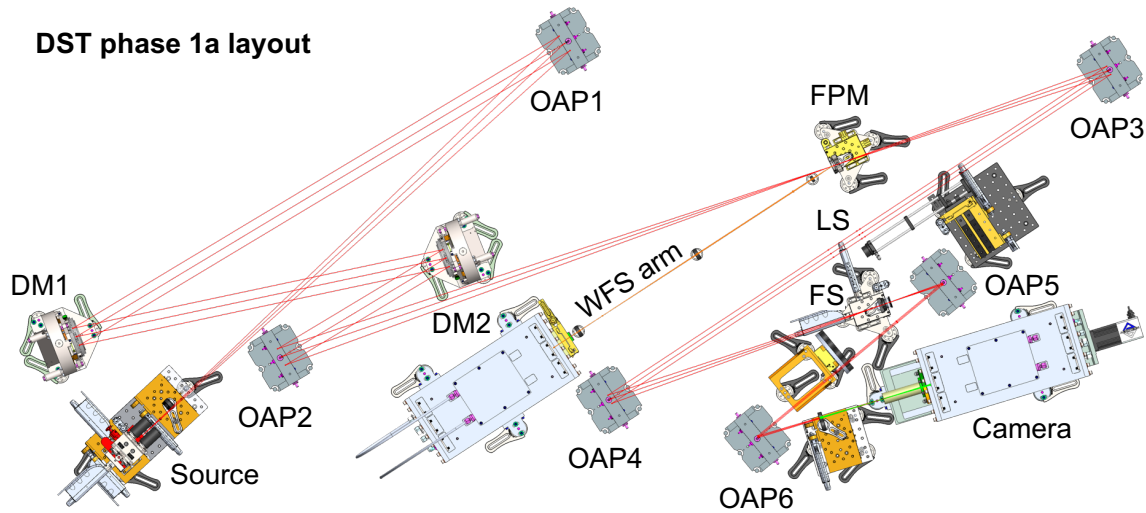
Figure 2. The DST phase 1a optical layout. Source: the star simulator. OAP: off-axis parabola. DM: deformable mirror. FPM: focal plane mask. LS: Lyot stop. FS: Field stop. Camera: imaging camera.
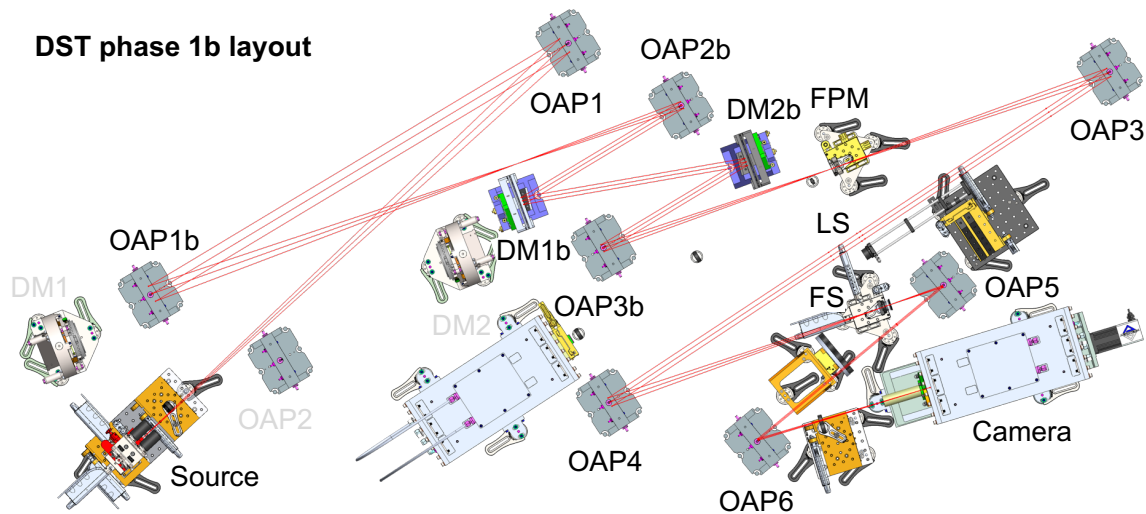
Figure 3. The DST phase 1b optical layout. Same as the phase 1a layout in Fig. 2, but OAP1b picks off the beam from its original path. OAP3b focuses the beam onto the FPM along its original path without modifying the focal ratio. Switching back to the phase 1a layout is possible by simply removing OAP1b and OAP3b.

Phase 2: Simulating a segmented pupil shape

- Choose preferred DM technology based on phase 1b. Revert to the phase 1a beam path (Fig. 2) by removing OAP1b and OAP3b, if necessary.

- Introduce a pupil mask that simulates obstructions due to segment gaps between OAP1 and DM1.

- Use best FPM from phase 1a.

- Goal: Demonstrate $<10^{-9}$ raw contrast levels in a 360° dark hole, 3-10 λ/D, and a spectral bandwidth of $\Delta\lambda/\lambda = 0.1$.
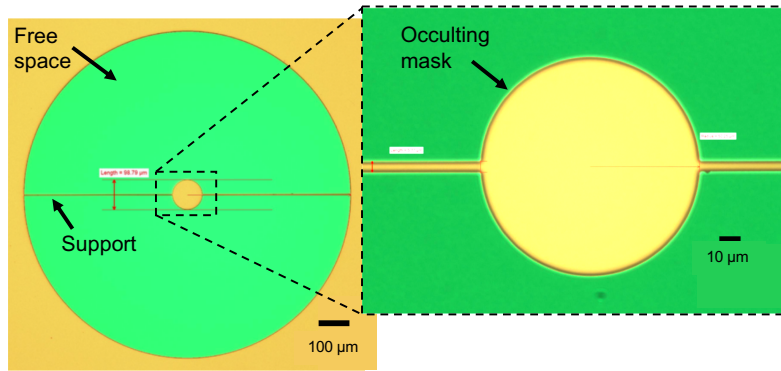
Figure 4. Microscope images of a freestanding silicon focal plane mask. The green regions are open area where light is transmitted. The outer diameter of the transmitting region is 1 mm, the inner diameter is 100 μm, and strut supporting the occultor is 5 μm wide.

Phase 3: Simulating dynamic disturbances
Phase 3a: Commission the reflective wavefront sensor (WFS) beam path

- Introduce a focal plane mask with a phase dimple to form a Zernike WFS sensitive to spatial frequencies up to at least $N_{\text{act}}/2$ cycles per pupil diameter.

- Goal: Demonstrate the measurement accuracy of changes in WFE of ~100 pm RMS.

- Stretch goal: Demonstrate improved dark hole stability at raw contrast $<10^{-9}$.

Phase 3b: Commission the disturbance source

- Introduce telescope simulator with capability to introduce low- and mid-spatial frequency errors that are representative of segment-to-segment piston and tip/tilt errors.

- Goal: Demonstrate that low-order and mid spatial frequency aberrations can be precisely injected upstream of the coronagraph at levels consistent with changes in raw contrast $<10^{-9}$.

- Stretch goal: Demonstrate that slowly varying aberrations injected by the disturbance source can be sensed and corrected in closed loop using the ZWFS.

## Exit criteria for commissioning phases

The DST team has defined exit criteria for each phase of the commissioning process that balances the achieved performance and prevents delays in schedule. A DST commissioning phase is complete if any of the following criteria are true:

1. **Raw contrast**: The quantified raw contrast (or similar) goal has been achieved.

2. **Justified error budget**: If the testbed converges to a raw contrast higher than the raw contrast goal in criterion 1, the error budget terms limiting performance have been clearly identified and quantified. In this case, assess possible remedies without violating criterion 3.

3. **Time limit**: The experiments surpass the time frame allotted by the ExEP office, which is nominally two months per phase. Extending any phase beyond two months will require a review by a group of external stakeholders.

Detailed description of experiments

Phase 1
Prior to the commissioning of DST, the first demonstration of raw contrast levels in the regime needed to image rocky exoplanets was by Trauger and Traub (2007)[4,5] who achieved 6×10^{-10} using a band-limited coronagraph and a single DM to generate a half plane dark hole within an angular separation range of 4-10 λ/D over a bandwidth of $\Delta\lambda/\lambda = 0.02$. Raw image contrasts of 3×10^{-10} over 2% bandwidths, 6×10^{-10} over 10% bandwidths, and 2×10^{-9} over 20% bandwidths around λ=800 nm were later demonstrated in half plane dark holes using a similar band-limited occultor[6]. In the context of WFIRST, "hybrid" Lyot
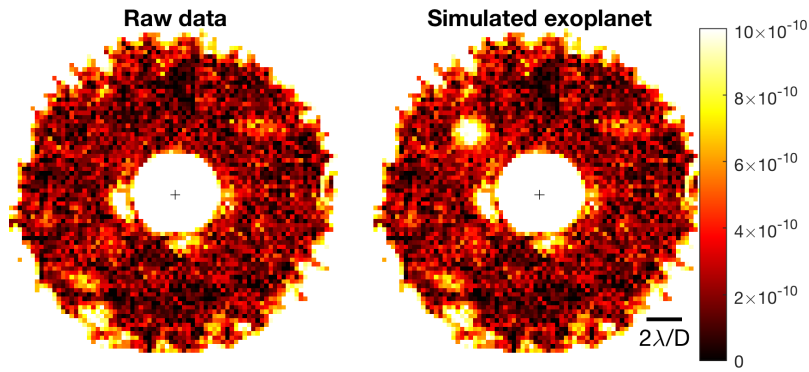
Figure 5. Monochromatic dark hole achieved during DST phase 1a. (*left*) Raw data after dark subtraction and normalized to the peak of the off-axis PSF. (*right*) Data with a fake companion injected at 5 λ/D in post-processing that is 10^{-9} times fainter than the simulated star.

coronagraph was demonstrated below 5×10^{-9} mean raw contrast with a 10% bandwidth centered at 550 nm in the 360° dark hole over an angular separation range of 3-9 λ/D[7]. Both of these ground-breaking demonstrations used vacuum testbeds at JPL/HCIT. DST builds upon this experience in order to achieve its phase 1a goals, which aim to improve on past demonstrations to demonstrate a noise floor on the order of 10^{-10} in an annular dark hole, 3-10 λ/D, with a spectral bandwidth of $\Delta\lambda/\lambda = 0.1$.

The focal plane masks (FPMs) available for DST commissioning are: (1) circular, quasi-opaque occulting spots formed by a disc of uniform nickel (optical density of 3.7) on BK7 or fused silica glass substrates and (2) freestanding silicon masks with aluminum coating (optical density >12), which allow for testing without a substrate (see Fig. 4). All have an effective angular radius of ~2.7 λ/D. The Lyot stop for both cases is a free-standing annulus with three evenly spaced radial struts supporting the central obscuration. The inner and outer diameters are 0.21 and 0.69 times that of the geometric pupil at the Lyot stop, which reduces the pupil area by a factor of ~0.43. The DMs used in phase 1a are manufactured by Xinetics Inc. with PMN electroceramic actuators in a 48×48 square array with an inter-actuator pitch of 1 mm. The inter-DM separation is 1 m.

Starting in fall of 2018, the phase 1a experiments[1] offered an opportunity to (1) align the primary beam path and confirm wavefront quality, (2) test the primary DST hardware, interfaces, and control software, (3) mitigate scattered light and other incoherent background sources, and (4) quantify the testbed stability. As of March 2019, the DST team achieved a mean raw contrast of 4.5×10^{-10} averaged over angular separations 3-9 λ/D with a bandwidth of $\Delta\lambda/\lambda = 0.1$ in a single polarization. With the same setup in monochromatic light, the deepest raw contrast was 2×10^{-10} with the same dark hole region (see Fig. 5). Testing coronagraphs in both monochromatic and polychromatic light provides a means to separate the limitations of the testbed hardware and coronagraph design.

	Error source	Contrast contribution
Testbed hardware	DM electronics	$\sim 1 \times 10^{-10}$
	Other incoherent background	$\sim 1 \times 10^{-10}$
Coronagraph design	FPM substrate ghost	$\sim 1 \times 10^{-10}$
	Coronagraph chromaticity	$\sim 1 \times 10^{-10}$
	Total:	4×10^{-10}

**Table 1.** Division of the DST error budget based on phase 1a experiments.

For the nickel-on-glass Lyot coronagraph and Xinetics DMs, the phase 1a experiments led to the error budget beak down given in Table 1. Since monochromatic light gives a raw contrast of 2×10^{-10}, we allocate that portion of the error budget to the testbed hardware itself. Approximately 1×10^{-10} is consistent with the contrast limits imposed by the DM electronics, which are 16 bit and provide a minimum step size in the DM surface height of 5.4 pm (see Fig. 6). There is an additional background of 1×10^{-10} attributed to stray light and imperfect detector calibration.

The design of the coronagraph increases the raw contrast by 2×10^{-10} above the estimated testbed floor. This is attributed to

---

[1]The details of the DST design, integration, and phase 1a experiments will be presented in the Proceedings of the SPIE, Techniques and Instrumentation for Detection of Exoplanets IX, August 2019. See K. Patterson et al. and B.-J. Seo et al., in preparation.
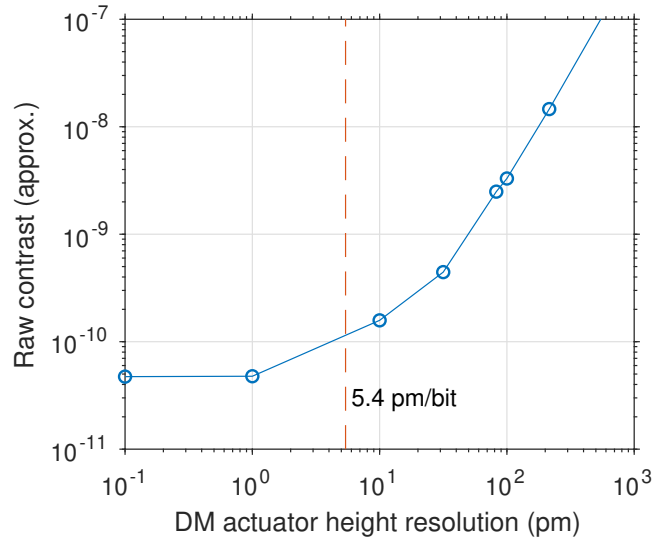
Figure 6. Raw contrast floor set by the DM surface height resolution based on numerical simulations of the DST by Daniel Echeverri (Caltech) using the FALCO software package[8].
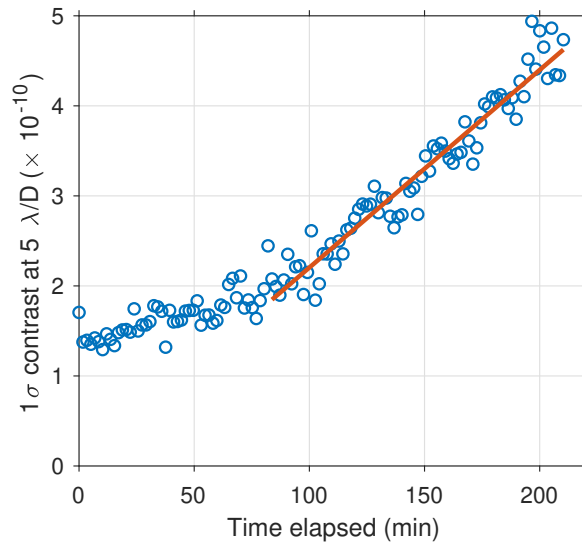

Figure 7. Raw contrast stability measurement. The speckle noise level at $5\,\lambda/D$ starts at 1×10^{-10} and increases by 1×10^{-10} per hour.

two effects. The first is the nonzero reflection from the FPM substrate surfaces. This "ghost" disappears in the monochromatic case due to the increase in coherence length. The second limitation is chromatic aberrations innate to the Lyot coronagraph design that are difficult to sense and correct using a discrete number of sub-bands during the wavefront control process. The freestanding occultor (Fig. 4) was designed to remove the substrate ghost, but did not improve overall performance likely because of additional wavelength-dependent diffraction from the outer boundary. Future studies may achieve better performance using a similar FPM with a larger outer diameter to mitigate both the ghost and coronagraph chromaticity.

After achieving the 2×10^{-10} dark hole in monochromatic light, the long term contrast stability of the testbed was measured empirically by taking continuous 100 sec exposures for a duration of 3.5 hr while keeping the testbed in a constant control state. As a representative measure, the raw speckle noise at $5\,\lambda/D$ was initially 1×10^{-10} and after an hour increased at a drift rate of 1×10^{-10} per hour (see Fig. 7).

As of March 2019, the exit criteria of phase 1a have been met. The raw contrast performance has converged on 4×10^{-10} and the error budget has been clearly justified. The team is preparing to move on to phase 1b and will work on specific upgrades in parallel to help reduce the testbed noise floor: (1) reduce the DM surface height resolution by increasing the bit depth of the
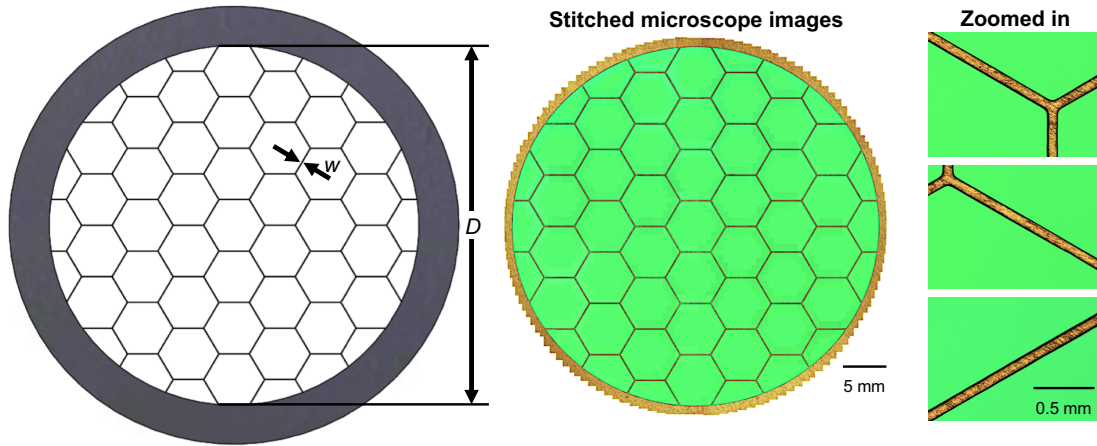
Figure 8. The DST phase 2 segmented pupil mask. (*left*) By design, the mask has a diameter is $D = 41.75$mm and the gap width, w, of 50-100 μm. (*middle*) Stitched microscope images of the mask and (*right*) zoomed in images on individual struts and junctions. The green regions are free space. Images courtesy of Simon Vuong and Bala Balasubramanian, JPL.
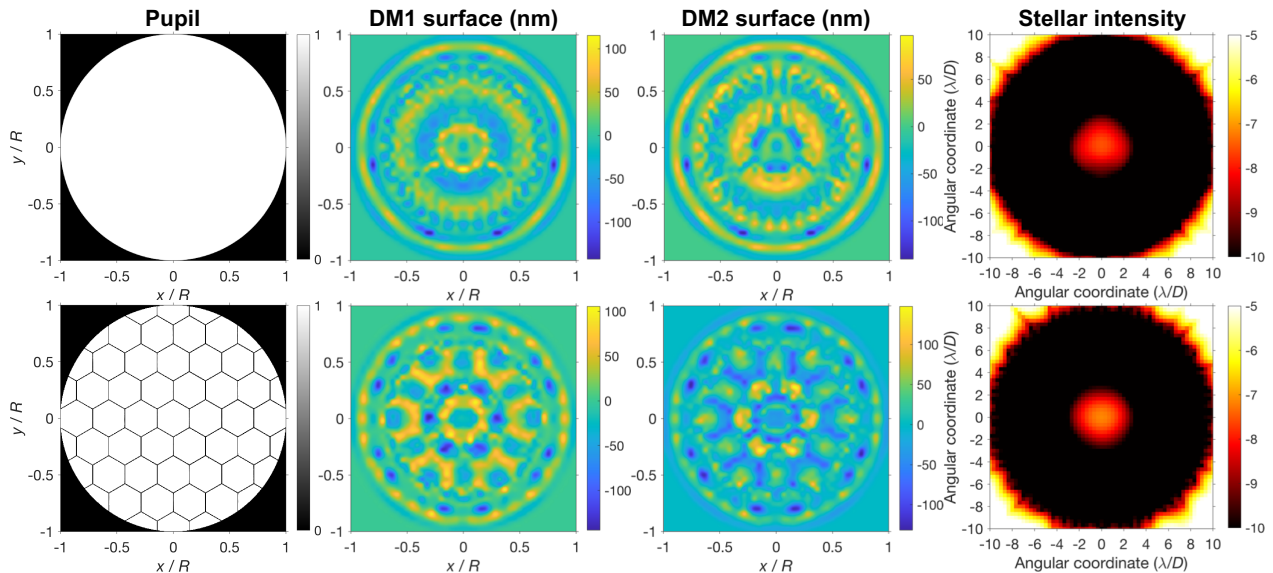

Figure 9. Simulation of the phase 2 experiment. *Left to right:* The pupil mask, DM shapes in nm, and normalized stellar intensity on a log scale for (*top row*) phase 1a and (*bottom row*) phase 1b. Change from the clear to the segmented aperture only requires modification to the DM shapes in theory. These simulations are based on measurements of the mask shown in Fig. 8.

driver electronics and (2) improve the baffling in the testbed for stray light control.

For Phase 1b, DST will be switched from the layout shown in Fig. 2 to Fig. 3. In doing so, the DST will be non-invasively modified to bypass the Xinetics DMs and use MEMS DMs from Boston Micromachines with 50 electrostatic actuators across, an inter-actuator pitch of 400 μm, and an DM separation of 0.6 m. Generally speaking, the advantage of the MEMS DMs is their stability. However, MEMS DMs have large periodic surface errors that may prevent coronagraphs from reaching 10^{-10} raw contrast. The currently available DM electronics for the MEMS DMs provide a minimum surface height change of $\sim$10 pm/bit (TBD), which is also expected to limit the raw contrast to $> 10^{-10}$. Thus, the raw contrast goal is set at 10^{-9} in order to validate these model predictions. Otherwise, the team will obey the exit criteria given above.

Phase 2
Phase 2 will introduce a pupil mask with linear obscurations that represent the discontinuities in a segmented aperture (see Fig. 8). The pupil mask has a transmissive design with a free standing structure to eliminate the need for a substrate. The
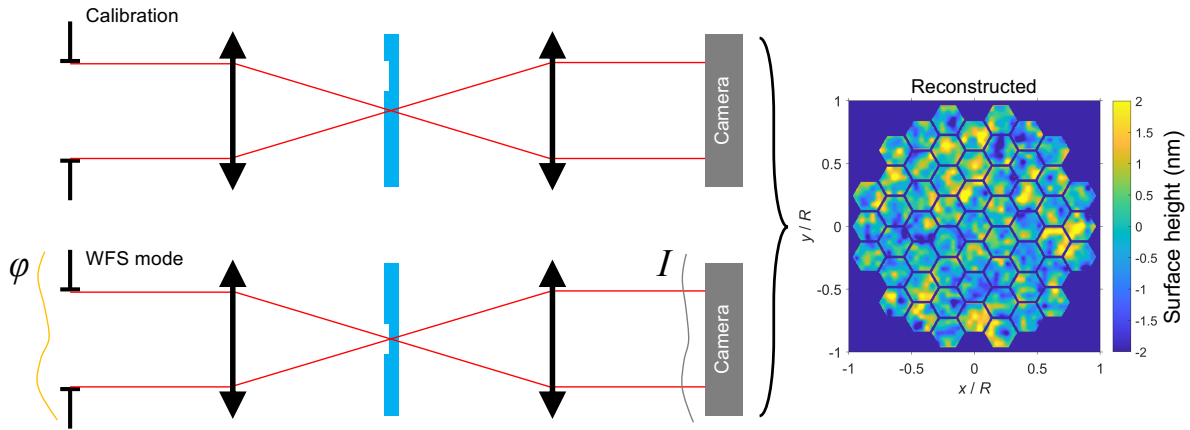
Figure 10. Unfolded Zernike wavefront sensor layout showing (*top*) the calibration configuration with the phase dimple misaligned and (*bottom*) the WFS configuration with the phase dimple aligned. These two images may be combined to reconstruct the wavefront.
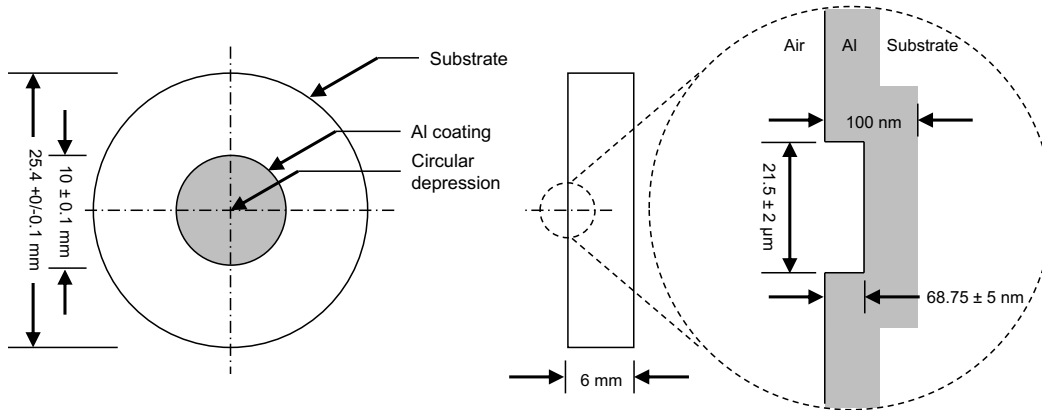
Figure 11. Schematic of the Zernike wavefront sensor commissioning mask. Starlight reflected off of the aluminum (Al) disk will make an image of the pupil on camera in the WFS arm (see Fig. 2). Zoomed-in region not to scale.

segmentation pattern is representative of the 8 m, off-axis, segmented, LUVOIR B architecture, which has seven hexagonal segments across the inscribed pupil diameter with a gap width of 6 mm ($<0.1\%$ of the pupil diameter). On DST, the pupil diameter is $D = 41.75$mm and the goal gap width, w, to match LUVOIR B is ~ 31 μm. To minimize manufacturing defects, the actual w that will be used on DST is 100 μm, or $3\times$ larger than expected for future segmented aperture space telescopes.

Phase 2 of commissioning is primarily intended to make sure the pupil masks are high enough quality for use in future experiments. However, it will also test the hypothesis that any dual-DM apodized coronagraphs demonstrated to achieve raw contrast of 10^{-10} on an unobstructed aperture will also achieve similar contrast on a segmented aperture provided the gaps are sufficiently small. Although the Lyot coronagraph used in phase 1a is expected to achieve similar contrast levels in phase 2 (see Fig. 9), the raw contrast goal has been relaxed to 10^{-9} for commissioning and otherwise shares the same exit criteria as phase 1a.

Phase 3

Phase 3 will first commission a wavefront sensor (WFS) and then a disturbance source for injecting wavefront errors in a controlled manner.

The WFS is required to detect spatial frequencies up to at least $N_{act}/2$ cycles per pupil diameter. The Zernike wavefront sensor (ZWFS)[9,10] is one of the most sensitive for such a large range of spatial frequencies. This is especially useful for monitoring the surface figure of the DMs and alignment of a segmented mirror[11,12], potentially to picometer precision[13]. The ZWFS will use the WFS arm shown in Fig. 2 by reflecting the starlight off of the focal plane mask. Figure 10 shows an unfolded version of the WFS arm to illustrate how the ZWFS works. First, a calibration image of the pupil is taken with the phase dimple

misaligned. Then, the phase dimple is aligned to the star to convert phase aberration into amplitude at the WFS camera. These two images are then combined to reconstruct the wavefront. The design of the DST ZWFS mask is shown in Fig. 11, which consists of a glass substrate with a circular depression coated in aluminimum to ensure high reflectively. Future coronagraphs may integrate the ZWFS phase dimple directly on the FPM.

The WFS arm commissioning will consist of installing the reflective ZWFS mask (Fig. 11), validating of the optical layout, and testing reconstruction algorithms for small changes in the wavefront. A lens of focal length 100 mm in the WFS arm will give 400 pixels across the pupil image. The sensitivity of the WFS will be determined empirically by repeatedly applying small changes to the DM and comparing the measured wavefront to the expected changes. The commissioning goal is to demonstrate measurement accuracy of changes in WFE of $\sim$100 pm RMS and potentially improved stability at raw contrast levels $<10^{-9}$.

The design of the disturbance source (phase 3b) is in preparation. It will consist of a mirror with tip/tilt control to introduce jitter and an additional deformable mirror for simulating other wavefront drifts. Given the aggressive timeline of planned experiments on DST and the importance of having DST in working order to make as much progress as possible prior to the conclusion of the Astro2020 decadal survey, the current plan is to build a second testbed with very similar design (DST-2) with additional relay optics to produce two new pupil planes upstream of the deformable mirrors. The design, integration, and commissioning of the DST-2 will be in parallel to the continued efforts on the original DST, soon to be called DST-1.

Future experiments on DST

In order to optimize the scientific yield of exoplanet surveys with a direct imaging mission, future coronagraph testing aims to maximize throughput, field of view, and bandwidth of coronagraphs at the 10^{-10} raw contrast level. Some examples are:

- Lyot coronagraphs developed as part of a project funded by the ExEP TDEM program (PI: John Trauger).

- Vortex coronagraphs being developed on the adjacent General Purpose Coronagraph Testbed (GPCT) as part of a TDEM (PI: Eugene Serabyn). Vortex coronagraphs[14,15] are the baseline design for the HabEx[16] and LUVOIR B[17] concepts.

- Apodized Pupil Lyot Coronagraph (APLC)[18,19] designs are baselined for the LUVOIR A concept[20] since they are better-suited for large, centrally-obscured telescope apertures. APLCs require an additional optical relay to create a reflective pupil plane and thus may be tested on the future DST-2.

- Phase induced amplitude apodization (PIAA) coronagraphs are high throughput, small inner working angle designs (potentially below $2\,\lambda/D$) that are limited in raw contrast. PIAA coronagraphs are useful for efficient large-wavelength characterization of planets detected near the visible inner working angle[21].

The full HCIT schedule is included at the end of this document for reference.

Acknowledgements

References

1. Gaudi, B. S. *et al.* The Habitable Exoplanet Observatory (HabEx) Mission Concept Study Interim Report. *ArXiv e-prints* 1809.09674 (2018).

2. The LUVOIR Team. The LUVOIR Mission Concept Study Interim Report. *ArXiv e-prints* 1809.09668 (2018).

3. Crill, B. & Siegler, N. Exoplanet Exploration Program Technology Plan Appendix 2019. https://exoplanets.nasa.gov/internal_resources/1123/.

4. Trauger, J. T. & Traub, W. A. A laboratory demonstration of the capability to image an Earth-like extrasolar planet. *Nature* **446**, 771–773, DOI: 10.1038/nature05729 (2007).

5. Trauger, J. *et al.* Laboratory demonstrations of high-contrast imaging for space coronagraphy. *Proc. SPIE* **6693**, 66930X, DOI: 10.1117/12.735004 (2007).

6. Trauger, J., Moody, D., Gordon, B., Krist, J. & Mawet, D. Complex apodization lyot coronagraphy for the direct imaging of exoplanet systems: design, fabrication, and laboratory demonstration. *Proc. SPIE* **8442**, 84424Q, DOI: 10.1117/12.926663 (2012).

7. Seo, B.-J. *et al.* Hybrid Lyot coronagraph for WFIRST: high-contrast broadband testbed demonstration. *Proc. SPIE* **10400**, 104000F, DOI: 10.1117/12.2274687 (2017).

8. Riggs, A. *et al.* Fast linearized coronagraph optimizer (FALCO) I: a software toolbox for rapid coronagraphic design and wavefront correction. *Proc. SPIE* **10698**, 106982V, DOI: 10.1117/12.2313812 (2018).

9. Bloemhof, E. E. & Wallace, J. K. Simple broadband implementation of a phase contrast wavefront sensor for adaptive optics. *Opt. Express* **12**, 6240–6245, DOI: 10.1364/OPEX.12.006240 (2004).

10. N'Diaye, M. *et al.* ZELDA, a Zernike wavefront sensor for the fine measurement of quasi-static aberrations in coronagraphic systems: concept studies and results with VLT/SPHERE. *Proc. SPIE* **9909**, 99096S, DOI: 10.1117/12.2232463 (2016).

11. Dohlen, K. *et al.* ZEUS: a cophasing sensor based on the Zernike phase contrast method. *Proc. SPIE* **6267**, 626734, DOI: 10.1117/12.671377 (2006).

12. Janin-Potiron, P. *et al.* Fine cophasing of segmented aperture telescopes with ZELDA, a Zernike wavefront sensor in the diffraction-limited regime. *Astron. Astrophys.* **603**, A23, DOI: 10.1051/0004-6361/201730686 (2017).

13. Moore, D. B. & Redding, D. C. Picometer differential wavefront metrology by nonlinear Zernike wavefront sensing for LUVOIR. *Proc. SPIE* **10698**, 1069841, DOI: 10.1117/12.2312600 (2018).

14. Mawet, D., Riaud, P., Absil, O. & Surdej, J. Annular Groove Phase Mask Coronagraph. *ApJ* **633**, 1191–1200, DOI: 10.1086/462409 (2005).

15. Foo, G., Palacios, D. M. & Swartzlander, G. A. Optical vortex coronagraph. *Opt. Lett.* **30**, 3308–3310, DOI: 10.1364/OL.30.003308 (2005).

16. Ruane, G., Mawet, D., Mennesson, B., Jewell, J. & Shaklan, S. Vortex coronagraphs for the Habitable Exoplanet Imaging Mission (HabEx) concept: theoretical performance and telescope requirements. *JATIS* **4**, 015004, DOI: 10.1117/1.JATIS.4.1.015004 (2018).

17. Ruane, G. *et al.* Fast linearized coronagraph optimizer (FALCO) IV: coronagraph design survey for obstructed and segmented apertures. *Proc. SPIE* **10698**, 106984U, DOI: 10.1117/12.2312973 (2018).

18. N'Diaye, M. *et al.* Apodized Pupil Lyot Coronagraphs for Arbitrary Apertures. V. Hybrid Shaped Pupil Designs for Imaging Earth-like planets with Future Space Observatories. *ApJ* **818**, 163, DOI: 10.3847/0004-637X/818/2/163 (2016).

19. Soummer, R. *et al.* High-contrast imager for complex aperture telescopes (HiCAT): 5. first results with segmented-aperture coronagraph and wavefront control. *Proc. SPIE* **10698**, 106981O, DOI: 10.1117/12.2314110 (2018).

20. Pueyo, L. *et al.* The LUVOIR architecture "A" coronagraph instrument. *Proc. SPIE* **10398**, 103980F, DOI: 10.1117/12.2274654 (2017).

21. Kern, B. *et al.* Phase-induced amplitude apodization complex mask coronagraph mask fabrication, characterization, and modeling for wfirst-afta. *JATIS* **2**, 1–8, DOI: 10.1117/1.JATIS.2.1.011014 (2016).

ExEP High Contrast Imaging Testbed Utilization Schedule

3/28/2019

Legend:
- ▬ Planned Activity
- ▨ Testbed Open
- ▮ TDEM Work
- ▬ Testbed Reconfiguration

Testbed Facilities	2018	2019	2020	2021

HCIT-1: WFIRST-OMC | WFIRST-ETB

HCIT-2w:
- [DMs 48.1 & 48.2] Reserved for WFIRST for additional coronagraph risk mitigation, performance opportunities, troubleshooting, and TRL-6 demonstration. Dedicated through LRD 2025.
- [DMs 48.3 & 48.4] Unobscured Demo; DST Phase I (HLC)
- 1/2 DST Phase I
- 2/28 3/15 CGI MEMS DM — DST Phase I Masks
- 7/1 DST Phase II
- 11/18 Trauger HLC (1 of 2)
- 2/14 3/14 Serabyn VC (4 of 4)
- 5/13 DST
- 12/1 12/30 Trauger HLC (2 of 2)
- 3/31 DST Phase IIIA
- 5/1

HCIT-2e:
- GPCT 32 AOX DM Testing w/ New Elex
- 3/1 Serabyn VC (3 of 4)
- 5/23 5/30 Belikov PIAA (1 of 6)
- 7/31 Belikov PIAA (2 of 6)
- 10/4 11/28 Belikov PIAA (3 of 6)
- 1/24 3/19 Belikov PIAA (4 of 6)
- 5/22 7/16 Belikov PIAA (5 of 6)
- 9/2 10/27 Belikov PIAA (6 of 6)
- 12/25 2/18

SVC:
- [DMs 48.3 & 48.4] Bierden MEMS DMs
- 12/1 5/15

Abbreviations:
- AOX: Northrop Grumman's AOA Xinetics
- CGI: Coronagraph Instrument
- DM: Deformable Mirror
- DST: Decadal Survey Testbed
- ETB: Engineering Testbed
- GPCT: General Purpose Coronagraph Testbed
- HCIT: High-Contrast Imaging Testbed
- HLC: Hybrid Lyot Coronagraph
- LRD: Launch Readiness Date
- MEM: Micro-electro-mechanical
- PIAA: Phase Induced Amplitude Apodization
- SVC: Strategic Vacuum Chamber
- TDEM: Technology Development for Exoplanet Missions
- TRL: Technology Readiness Level
- VC: Vortex Coronagraph
- WFIRST: Wide-Field Infrared Survey Telescope